

Domain engineering in LiNbO₃ for tailoring the electro-optic response of waveguide modulators

Davide Janner (1), Michele Belmonte (2) and Valerio Pruneri (1, 3)

1) ICFO -Institut de Ciències Fotòniques, Mediterranean Technology Park. Av. del Canal Olímpic s/n 08860 Castelldefels, Barcelona, Spain. valerio.pruneri@icfo.es 2) Avanex Corporation Sede Secondaria, San Donato Milanese (MI), Italy 3) ICREA -Institutió Catalana de Recerca i Estudis Avançats, 08010, Barcelona, Spain

Abstract: *A general approach is proposed to achieve a predefined electro-optic response in domain inverted LiNbO₃ modulators. In particular an apodised domain inversion profile is used in a non-velocity matched configuration to obtain modulation with intrinsic third-order Bessel optical filtering for duobinary transmission.*

Introduction

With the increasing demand for broadband communication, optical networks play a crucial role as the primary carrier of the data stream. In this context, high-speed optical modulators are essential for optical transmission systems and external LiNbO₃ modulators are still extremely effective [1], in particular for long haul and metro applications, as it is shown by their recent increasing commercial demand. With respect to semiconductor materials, LiNbO₃ based modulators market share could even become larger if performance, integration and cost effectiveness further improve.

The basic scheme of an interferometric Mach-Zehnder amplitude modulator in a single domain crystal produces a frequency response which has a cardinal sine shape and a limited bandwidth inversely proportional to the length [1]. This feature represents a drawback in the picture of actual needs for broadband modulation because of the restriction of the bandwidth and because the ripples in the electro-optic (EO) response may negatively affect some transmission formats, e.g. duo-binary.

Domain inversion (DI) in ferroelectrics, such as LiNbO₃, produces a sign reversal of the second-order nonlinear optical properties, including the nonlinear optical coefficient and electro-optic coefficient [2]. So far its use in electro-optics, where one of the interacting fields is at low frequency or a microwave, has been mostly limited to quasi-velocity-matching devices using periodic structures to produce narrow band modulation at high frequency [3,4]. More recently domain inversion has been used to produce large bandwidth and low driving voltage modulation [5, 6], a desired chirp value for the output electro-optic modulated optical wave [7] and to realize single-side-band modulators [8]. When DI (also called poling) is used in a periodic fashion it allows

centering the EO frequency response of interest by simply changing the periodicity of the poling. In this case a quasi velocity matching condition is reached and the center of the cardinal sine is shifted from DC of the single domain (unpoled) modulator to the desired frequency, while its shape remains qualitatively the same. In the attempt of keeping the advantages of periodically poled modulators while broadening the bandwidth, multi period structures, constituted by a sequence of different period periodically poled zones, have been employed with promising results [9].

Using a new approach and considering general aperiodic poling profiles, we propose a DI configuration to tailor the EO response to a predefined one. In particular, we design an apodised longitudinal poling profile in non velocity matched (NVM) modulators to achieve a desired electro-optic response using an apodisation technique similar to that of fibre Bragg Gratings. As an example, we demonstrate the possibility to induce a predefined EO frequency response by reporting the synthesis of a third-order Bessel type modulation. This Bessel type modulator, embedding a filter at optical level, is suitable for duobinary transmission [10], without the need of any additional electrical filter in the transmitter.

Precise electro-optic response modulator

Let us consider a travelling wave z-cut LiNbO₃ modulator in NVM configuration, with straight electrodes and perfectly impedance matched [1]. In such a modulator the driving voltage is described by

$$V(x, t) = V_0 \sin(k_m \cdot \delta \cdot x - 2\pi f_m t_0) \quad (1)$$

where V_0 is the amplitude of the wave, $k_m = 2\pi n_m / \lambda_m$, is the microwave wave-number, $\delta = 1 - n_o / n_m$ is the relative mismatch between the refractive index of the microwave (n_m) and optical (n_o) waves, f_m is the microwave frequency corresponding to the wavenumber k_m and t_0 accounts for an initial phase. Driven by this wave, the phase change which the optical wave accumulates at the end of the modulator arms can be written as

$$\Delta\phi(t_0) = \int_0^L -\frac{2\pi n_0^3}{\lambda} r \frac{\Gamma}{2G} \cdot \{p(x) \cdot V_0 \sin[k_m \cdot \delta \cdot x - 2\pi f_m t_0]\} dx \quad (2)$$

where L is the length of the arms, λ is the optical wavelength, n_0 is the optical refractive index, r is the electro-optic coefficient (in our case, $r=r_{33}$), G is the spatial gap between the two electrodes and Γ is the overlap integral between the optical and microwave electric fields.

If we consider the following identity

$$P(f) = e^{j2\pi f x} \int_{-\infty}^{+\infty} p(x) \cdot e^{-j2\pi f x} dx = \int_{-\infty}^{+\infty} p(x) \cdot \cos(2\pi f x - 2\pi f t_0) - j \int_{-\infty}^{+\infty} p(x) \cdot \sin(2\pi f x - 2\pi f t_0) \quad (3)$$

we note that its imaginary part is very similar to Eq. 2 provided we extend the integration domain to infinity and introduce a rectangular window function to account for the finiteness of the poled region. Thus, we may write the phase change in Eq. 2 in terms of the Fourier transform of the poling function as

$$\Delta\phi'(t_0) = \frac{2\pi n_0^3}{\lambda} r \frac{\Gamma}{2g} V_0 \cdot \text{Im}\langle F[p(x)] \cdot e^{j2\pi f t_0} \rangle \quad (4)$$

in which the constants have the same meaning as in Eq. 2 and the symbol F denotes the Fourier transform of the windowed poling function $p(x)$. In this way, the response of the modulator can be obtained numerically via a simple Fast Fourier transform (FFT) of the poling function, and the relationship between the modulation frequency and the computed frequency of the FFT is given by:

$$k_m \cdot \delta = 2\pi f \rightarrow f_m = \frac{c}{N \cdot \Delta x \cdot \Delta n} l, \Delta f = \frac{c}{N \cdot \Delta x \cdot \Delta n}, \quad (5)$$

where N is the number of discrete samples into which is divided the poling function $p(x)$, Δx is the width of one sample, l is an integer number ranging from 0 to $N-1$, $\Delta n = n_m - n_0$ is the index mismatch, and Δf is the frequency step.

We also note that electrical losses of the modulating wave may be easily included in the computation by the substitution $p(x) \rightarrow e^{-\alpha x} p(x)$ in Eq. 4. Here, we

assume the loss parameter to be $\alpha(f) = k\sqrt{f}$ with $k=0.51$ (cm GHz)^{-1/2}. This value is obtained by fitting the losses of a typical modulator up to 40GHz computed using FEM techniques.

The advantage of the formulation of Eq. 4 for the modulator response is that a straightforward inversion could be obtained by the simple relation:

$$h(x) = \text{Re}\langle F^{-1}[\Delta\phi_0(f)] \rangle, \quad (6)$$

where F^{-1} is the inverse Fourier transform and $\Delta\phi_0(f)$ is the desired frequency response of the modulator so that we may recover a continuous pol-

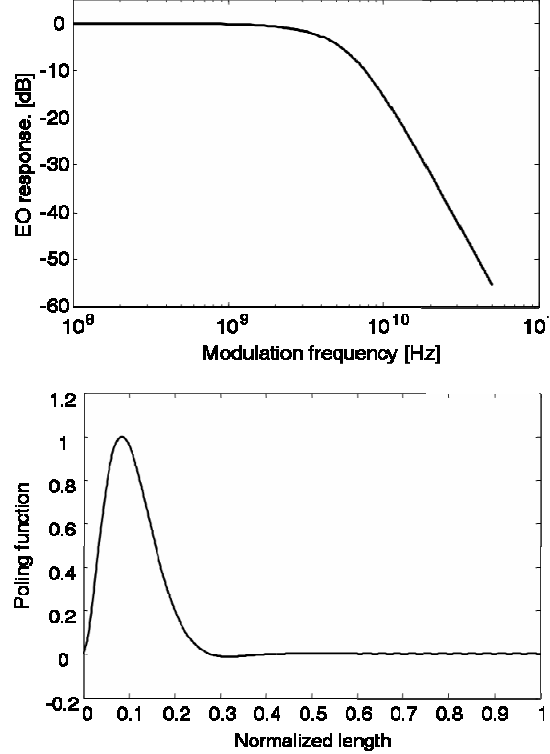


Fig. 1: Desired electro-optic response for a third order Bessel filtering modulator with a -3 dB frequency of 4.5 GHz (top). Reconstructed poling function $h(x)$ which produces the desired Bessel filter response. (bottom)

ing function from a desired frequency response. Also in this case a common FFT algorithm can be employed, and with analogous consideration as in the direct case, the following relationships can be obtained:

$$\Delta x = \frac{c}{N \cdot \Delta f \cdot \Delta n} \quad L = N \Delta x = \frac{c}{\Delta f \cdot \Delta n} \quad (7)$$

where Δx is the spatial step into which the poling function $h(x)$ is sampled, N is the number of discrete samples considered, Δf is the step in frequency, Δn is the index mismatch, and L is the total length of the modulator.

The function $h(x)$ in Eq. 6 is a continuous function assuming values ranging from -1 to +1. For this reason, in order to recover the real apodised poling profile $p(x)$ which assumes only two discrete values (-1 or +1), we must provide an algorithm to quantize the continuous function $h(x)$. The procedure is analogous to the apodisation technique used in fiber Bragg grating design.

Let us divide the domain of the function $h(x)$ into a large number of sections of length L_s and consider also the target poling function $p(x)$ composed by equally spaced sub-domains each of size L_s/N , where $N>1$ is an integer. After computing \bar{h}_i , the average of $h(x)$ on the i -th section, we can convert it in terms of

the poling function $p(x)$ by letting the average value of $p(x)$ on that section coincide with \bar{h}_i . For example, if we assume for a single section that $\bar{h}_i = -0.4$, this means that 30% of the sub-domains comprised by $p(x)$ in that section must be set to +1 and the other 70% of the poling sub-domains must be set to -1, so that $0.3 \cdot 1 + 0.7 \cdot (-1) = -0.4$. In this way, the mean value \bar{h}_i of the continuous function $h(x)$ is easily reported to the poling function $p(x)$ by simply imposing a length $L_p^- = 0.7L_s$ of the section to -1 and a length $L_p^+ = 0.3L_s$ to +1.

This approximation is valid since we assumed the section length L_s much smaller compared to the coherence length ($\lambda_m/2\Delta n$, about 750 μm at 10 GHz), of the microwave and the phase modulation in this case has an almost linear response with no sensitivity on the order of the sub-domains of $p(x)$ in the single section.

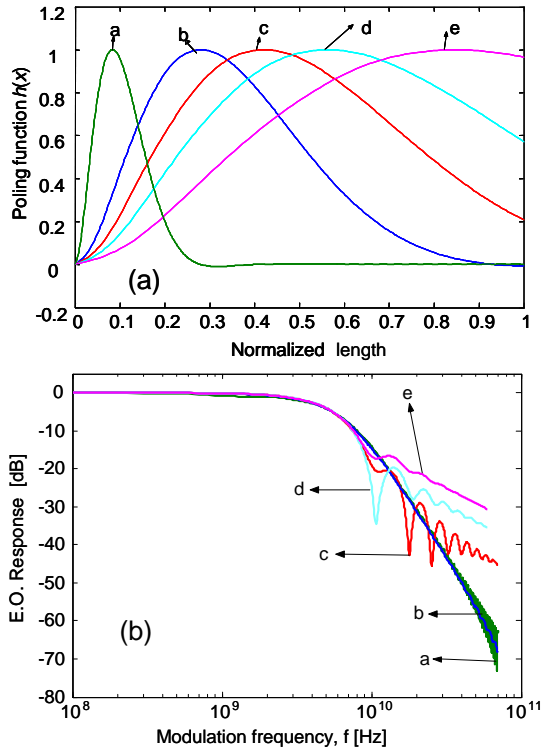


Fig. 2: Comparison of the different poling functions (fig. a) and their E. O. response (fig. b) for the a) ideal case ($V_\pi=99$ V·cm) or truncated to b) the first lobe ($V_\pi=30$ V·cm); c) 2/3 of the first lobe ($V_\pi=21$ V·cm); d) 1/2 of the first lobe ($V_\pi=18.6$ V·cm); e) 1/3 of the first lobe ($V_\pi=20.1$ V·cm).

To illustrate the potential of this technique, we report here, as an example, a modulator having an EO response of a third order Bessel filter with a -6 dB frequency of 6 GHz. This kind of filter is very useful in the duobinary format transmissions where the tails of the typical cardinal sine response of normal modula-

tors has negative effects and an electrical filter is usually needed to cut them off [10]. Starting from the desired EO response and applying the inverse Fourier transform algorithm of Eq. 6, we obtain the continuous poling profile $h(x)$ as reported in figure 1. The poling function here is plotted against a normalized length $L' = \Delta n \cdot L$ since, in this first stage of the design, we neglect the microwave losses and assume that the EO response does not depend on the length by keeping the product $\Delta n \cdot L$ constant. In such a way, we can consider the length L and the index mismatch Δn design parameters to be decided *a posteriori* depending on the EO response and including the microwave losses. Observing the recovered poling function in figure 1, we note that the longest part of it is nearly zero, almost not influencing the modulation of the phase. Moreover, the average of the function $h(x)$ over the domain can be used to estimate $V_\pi = 99$ V·cm which is extremely large. Thus, from these considerations we can argue that the last part of the poling function which is nearly zero could be disregarded in the modulator design and dropped.

To address this point in figures 2(a)-(b) we report the comparison of the ideal and some poling functions obtained by truncation of the ideal one and their respective EO responses. We note that the switching voltage is inversely proportional to the area under the poling curve and moreover the more truncated the poling function the worse the EO response (ripples). From figure 5(b) we may also note that the closest response to the ideal case of the third order Bessel filter is the function truncated at the first lobe differentiating its response from the ideal one only by negligible ripples at higher frequencies. Moreover, this profile has a much lower $V_\pi = 30$ V·cm.

Once chosen the single lobe function as our poling function, we may account for electrical losses. If we compare the EO responses with and without microwave loss, for a constant $\Delta n \cdot L$, we note that they depend on the device length. Indeed, with respect to the ideal (no microwave loss) EO response, the behaviour that accounts for the loss ($\alpha=0.49 \sqrt{f}$ dB/cm) for a modulator of length $L=45$ mm and $\Delta n=1.32$ remains qualitatively the same with the exception of the cut-off frequency that, from the 6 GHz ideal case, is reduced to about 5.25 GHz. However, the 6 GHz bandwidth could be achieved by initially designing the ideal structure (no losses) having a larger cut-off frequency, so that, after accounting for microwave loss, the EO response becomes the desired one.

The final apodised poling profile $p(x)$ for the designed Bessel type modulator with a cutoff frequency at -6 dB of 6 GHz is reported in figure 3 and compared with the continuous poling function $h(x)$. Such a modulator has a switching voltage of 6.6 V and the EO response for the poling profile calculated is com-

pared to the ideal case of a Bessel third order filter in figure 4 showing a good agreement and the effectiveness of the method.

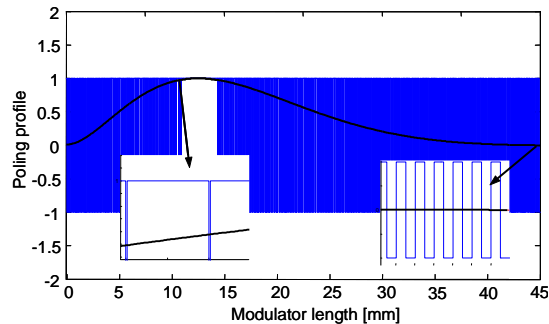


Fig. 3: Continuous poling function (black solid) and reconstructed discrete valued profile function (blue line).

The proposed design is for a modulator that can be used for a 10 Gb/s transmission. The common approach consists in 3rd order Bessel type electrical filtering of a standard 10Gb/s modulator (>10GHz bandwidth) which results in a typical driving voltage in the 4 to 5 V range. Note that, in comparison, the driving voltage in our case is higher but could be reduced by increasing the transverse overlap (Γ) which, in the case of classical modulators, would not be possible because the VM condition imposes severe geometrical constraints.

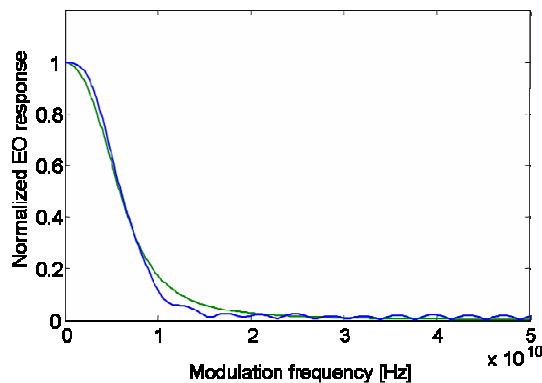


Fig. 4: Comparison of the normalized EO response of the ideal (green) and truncated (blue) poling function

Conclusions

The DI engineering procedure we proposed for precise EO response design is general and straightforward, requiring only simple numerical operations as an inverse Fourier transform and a small number of empirical tries providing precise results. No particular geometry of the electrodes is required, only straight lines, thus avoiding curvatures which cause reflections or the modification of the Γ coefficients; effects that can induce different phase changes in the two branches of the modulator producing residual chirp. Moreover, the possibility of tailoring the de-

sired EO response and integrate optical filtering (such as 3rd order Bessel) makes this technique powerful for design of commercial modulators.

References

1. E. L. Wooten, K. M. Kissa, A. Yi-Yan, E. J. Murphy, D. A. Lafaw, P. F. Hallemeier, D. Maack, D. V. Attanasio, D. J. Fritz, G. J. McBrien, D. E. Bossi, IEEE J. Select. Topics Quant. El., vol. 6, no. 1, pp. 69-81, Feb. 2000
2. R. S. Weiss and T.K. Gaylord, Appl. Phys. A, vol. 37, no. 4, pp. 191-203, 1985.
3. J.H. Schaffner, US patent 5,278,924 (1994).
4. Y. Lu, M. Xiao and G. J. Salamo, Appl. Phys. Lett., vol. 78, no. 8, pp. 1035-1037, 19 Feb 2001
5. V. Pruneri and A. Nespola, US patent 6,760,493, year 2004.
F. Lucchi, M. Belmonte, S. Balsamo, M. Villa, L. Trevisan, S. Pensa, G. Consonni, C. Emanuele, P. Vergani, M. Sottocorno, V. Pruneri, paper OWH3, to be presented at OFC 07.
6. S. Oikawa, F. Yamamoto, J. Ichikawa, S. Kurimura, K. Kitamura, J. Light. Tech., vol. 23, no. 9, pp. 2756-2760, Sep. 2005
7. N. Courjal, H. Porte, J. Hauden, P. Mollier and N. Grossard, J. Lightwave Tech., vol. 22, no. 5, pp. 1338-1343, May 2004.
8. H. Murata and Y. Okamura, in Photonics Based on Wavelength Integration and Manipulation, pp. 213-224, IPAP Books 2, 2005
9. Chen XF, Zeng XL, Chen YP, Xia YX, Chen YL, Journal. of Opt. A-Pure and applied optics, vol. 5, no. 3, pp. 159-162, May 2003
10. P. Bravetti, L. Moller, IEEE Phot. Tech. Lett., vol. 16, no. 9, pp. 2159 – 2161, Sept. 2004